Clim Dyn (2010) 35:1373–1391
DOI 10.1007/s00382-010-0767-5

# Application of blocking diagnosis methods to General Circulation Models. Part I: a novel detection scheme

**D. Barriopedro · R. García-Herrera · R. M. Trigo**

Received: 24 March 2009 / Accepted: 10 February 2010 / Published online: 3 March 2010


**Abstract** This paper aims to provide a new blocking definition with applicability to observations and model simulations. An updated review of previous blocking detection indices is provided and some of their implications and caveats discussed. A novel blocking index is proposed by reconciling two traditional approaches based on anomaly and absolute flows. Blocks are considered from a complementary perspective as a signature in the anomalous height field capable of reversing the meridional jet-based height gradient in the total flow. The method succeeds in identifying 2-D persistent anomalies associated to a weather regime in the total flow with blockage of the westerlies. The new index accounts for the duration, intensity, extension, propagation, and spatial structure of a blocking event. In spite of its increased complexity, the detection efficiency of the method is improved without hampering the computational time. Furthermore, some misleading identification problems and artificial assumptions resulting from previous single blocking indices are avoided with the new approach. The characteristics of blocking for 40 years of reanalysis (1950–1989) over the Northern Hemisphere are described from the perspective of the new definition and compared to those resulting from two standard blocking indices and different critical thresholds. As compared to single approaches, the novel index shows a better agreement with reported proxies of blocking activity, namely climatological regions of simultaneous wave amplification and maximum band-pass filtered height standard deviation. An additional asset of the method is its adaptability to different data sets. As critical thresholds are specific of the data set employed, the method is useful for observations and model simulations of different resolutions, temporal lengths and time variant basic states, optimizing its value as a tool for model validation. Special attention has been paid on the devise of an objective scheme easily applicable to General Circulation Models where observational thresholds may be unsuitable due to the presence of model bias. Part II of this study deals with a specific implementation of this novel method to simulations of the ECHO-G global climate model.

**Keywords** Atmospheric blocking · Automatic methods · Climate variability · Climate change · Reanalyses · General Circulation Models

D. Barriopedro (✉) · R. M. Trigo
CGUL-IDL, Faculdade de Ciências, Ed. C-8,
Universidade de Lisboa, Campo Grande,
Lisbon 1749-016, Portugal
e-mail: dbarriopedro@fc.ul.pt

D. Barriopedro
Departamento de Física, Facultad de Ciencias,
Universidad de Extremadura, Badajoz, Spain

R. García-Herrera
Departamento de Física de la Tierra II, Facultad de C.C. Físicas,
Universidad Complutense de Madrid, Madrid, Spain

## 1 Introduction

In addition to the quasi-stationary planetary scale circulation, the mid-latitude climate is dominated by transient synoptic disturbances co-existing with less common but persistent circulation patterns. Since these weather systems exhibit preferred spatial distributions, a significant modification in their amplitude, frequency and/or location (by either anthropogenic causes or natural variability) can lead to substantial changes in regional climates. As a consequence, an adequate representation of these systems is vital to model accurately the mid-latitude climate and to provide

credible projections in climate change scenarios. Among these weather systems, blocking is a classical subject in the meteorological literature that has captured the interest of the scientific community for several decades. The term was first introduced by meteorologists in the early twentieth century when referring to those weather situations in which the normal zonal flow was temporarily suppressed in a sector by strong persistent meridional type flow, thus "blocking" (i.e. interrupting) the normal west-to-east progress of extratropical migratory cyclone systems. Although there is no universally accepted blocking definition several features are widely recognized:

1. Blocking is characterized by a large-scale high pressure system with an anticyclonic circulation dominating the troposphere in the region where the prevailing westerlies are usually located. This can arise under two typical configurations: a high-low dipole structure that splits the jet into two branches north and south of the blocking high (diffluent or dipole block, Rex 1950a) or an amplified ridge with an omega-like shape (omega block, Sumner 1954). Under both situations, the high pressure is linked to the simultaneous occurrence of low pressure systems at lower latitudes either in the equatorial side of the diffluent block or upstream/downstream of the omega block.
2. Blocks are regional phenomena with a characteristic spatial dimension typical of the large-scale (e.g. Liu 1994). Unlike other features of the general circulation, they are quasi-stationary with lifetimes amounting from several days to 4 or 5 weeks (e.g. Knox and Hay 1984; Wiedenmann et al. 2002), thus being an important component of intraseasonal variability (Trenberth et al. 2007).
3. There are two preferred regions for blocking occurrence in the eastern sides of the Atlantic and Pacific oceans, coinciding with the climatological areas of wave amplification and the exit zones of the two main storm tracks. Although there is not yet a satisfactory dynamical theory of the blocking phenomenon, it is recognized that blocking onset, development and maintenance is influenced by large-scale waves, small scale perturbations and their mutual interactions (e.g. Charney and DeVore 1979; Tsou and Smith 1990; Nakamura et al. 1997). As a consequence, blocks can be detected through the whole year but exhibit seasonal variability with maximum occurrence in winter and spring (e.g. Tibaldi et al. 1994). At longer time scales, interannual and interdecadal variations are associated, though not tightly coupled (Stan and Strauss 2007), to oscillations of the main regional modes of low-frequency variability in the Atlantic and the Pacific, including the North Atlantic Oscillation (NAO, e.g. Barriopedro et al. 2006), El Niño–Southern Oscillation (ENSO, e.g. Wiedenmann et al. 2002) and the Pacific North America pattern (PNA, e.g. Croci-Maspoli et al. 2007). In addition, long-term memory components of the climate system such as sea surface temperatures (SSTs, Chen and Yoon 2002; Huang et al. 2002; Luo and Wan 2005) and snow cover conditions (García-Herrera and Barriopedro 2006) can modulate blocking occurrence. External forcings such as solar activity also exert a significant impact on blocking activity (Barriopedro et al. 2008).
4. Blocking occurrence is associated with anomalous weather conditions over long periods of time and large areas of mid and high latitudes, which can have major impacts on society. Synoptically, regions under the blocking high experience long periods of cloudless weather and drying conditions (e.g. Treidl et al. 1981). If the event is persistent, the long-lasting anomalies under the blocking high can be responsible for extreme events (Quiroz 1984; García-Herrera et al. 2007). Climatologically, blocks induce anomalous warm (cold) temperature anomalies upstream (downstream) of the blocking high due to the southerly (northerly) advection by the anomalous meridional flow. Westerly winds are replaced by easterlies and hence, the mean cyclone track and precipitation patterns are diverted toward polar or subtropical latitudes (Rex 1951; Trigo et al. 2004; Carrera et al. 2004).

A definition of blocking has become in itself a major issue, with different blocking indices focusing on different characteristics of the blocks. Albeit many blocking situations are successfully detected by any of the existing indices, there are some discrepancies in the reported frequency and location that may have consequences in observational and modelling studies (Doblas-Reyes et al. 2002). This has motivated a vivid debate on the type of features identified by each index and the most suitable method in providing a realistic approximation to blocking. The complexity of diagnosing blocking in automatic algorithms and the lack of agreement for a blocking definition has undermined the number of publications addressing blocking behaviour in General Circulation Models (GCMs, e.g. D'Andrea et al. 1998), as compared with those focusing on observational data. The main objectives of this paper (Paper I hereinafter) and the work presented in a companion paper (Paper II hereinafter) are twofold: (1) to present a novel blocking index that combines the most traditional approaches employed for blocking identification and overcomes some problems resulting from single methodologies; (2) to produce a blocking algorithm with applicability to observations and

long-term model simulations of different resolution and hence a tool for model validation and assessment of model response in past or future climate change scenarios.

Because of the lengthy nature of this analysis the paper is divided in two parts. Paper I deals with the design of the automatic method and its diagnosis in observational data. Paper II focuses on the applicability of the method as a tool for testing model performance. Paper I is organized as follows: Sect. 2 reviews previous blocking definitions. In Sect. 3 a novel approach is presented. Data, sources and a detailed description of the diagnostic method are also given. Section 4 presents a new 40-year blocking climatology for the Northern Hemisphere (NH), highlighting its differences with those resulting from different blocking definitions and thresholds. In Sect. 5, some concluding remarks and the outline of Paper II are summarized.

## 2 Blocking detection methods

### 2.1 Review

The long list of relevant literature about blocking discloses a broad diversity of detection methods. In most of them the identification of blocking events is made by demanding a minimum spatial extension and a temporal duration criteria to the blocked flows diagnosed on a daily basis. However, methodologies vary in many aspects, namely with respect to: (1) the sophistication involved in the methodology, (2) the base field, and, to a large degree, (3) the specific features of blocking employed for the daily identification (the so-called blocking index). Thus, blocking detection methods can be categorized in different ways attending to the objectivity of the procedure, the nature and type of the base field and the specific index used to diagnose blocking (Fig. 1).

The former classifies the methods into subjective and objective, depending on whether the decision is made by visual inspection or by an automatic routine. Some studies have developed a combined approach of both criteria (e.g. Lupo and Smith 1995).

There have been two traditional approaches concerning the nature of the base field: absolute meteorological fields or, alternatively, departures from a local, zonal or regional climatological mean. In both cases, the most common indicator is the geopotential height at 500 hPa (Z500). Other approaches use the meridional wind component (Kaas and Branstator 1993) or the local stream function

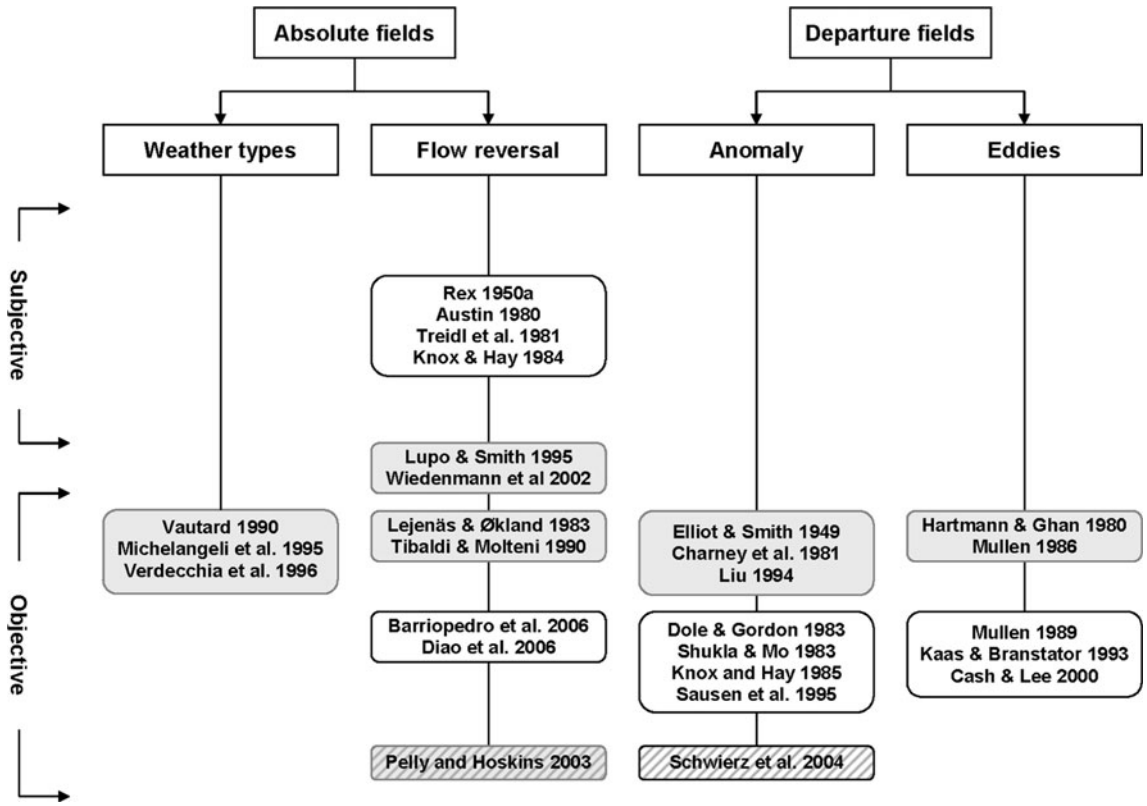


**Fig. 1** Review of blocking detection methodologies. Classification of blocking detection methods reported in the literature as a function of the objectivity (*left rows*), the nature of the base field (*header columns*) and the specific blocking index (*sub header columns*). *Shaded* (*not shaded*) *boxes* indicate methodologies that provide 1-D (2-D) descriptions of the blocked flow or indices of regional blocking-pattern activity. *Dashed* (*not dashed*) *boxes* are methods based on dynamical (standard isobaric) variables

computed in spherical harmonics expansion (Metz 1986). Alternatively, recent studies have employed dynamical parameters, including the vertically averaged potential vorticity (e.g. Schwierz et al. 2004) or the potential temperature on a dynamical tropopause, identified by a constant potential vorticity surface (e.g. Pelly and Hoskins 2003).

Finally, blocking methods can be further divided by the specific index used to catalogue blocking situations (i.e. the blocking definition). Thus, blocking events have been defined as: (1) regional and persistent meridional gradient reversals in the absolute geopotential height (or in the potential temperature) field, that reflect easterly geostrophic flows around a reference latitude representative of the jet stream (e.g. Lejenäs and Økland 1983; Tibaldi and Molteni 1990; Pelly and Hoskins 2003; Barriopedro et al. 2006; Diao et al. 2006); (2) persistent positive (negative) departures from the climatological height (potential vorticity) field (e.g. Dole and Gordon 1983; Shukla and Mo 1983; Knox and Hay 1985; Sausen et al. 1995; Schwierz et al. 2004); (3) eddy fields identified as regions bounded by a southerly (northerly) wind upstream (downstream) (Kaas and Branstator 1993; Cash and Lee 2000) or as areas where the height field strongly exceeds the zonal mean in a surrounding sector (Hartmann and Ghan 1980; Mullen 1986, 1989); (4) objective atmospheric circulation patterns derived from either statistical multivariate methods of weather regimes classification (Vautard 1990; Michelangeli et al. 1995) or neuronal networks (Verdecchia et al. 1996).

The indices of Dole and Gordon (1983), hereafter DG, and Tibaldi and Molteni (1990), hereafter TM, are the most commonly used characterizations of blocking, and they follow the pioneering studies of Elliot and Smith (1949) and Rex (1950a), respectively. Elliot and Smith (1949) identified blocking as sea level pressure (SLP) anomalies from the climatological mean exceeding a given threshold for a certain time. One year later, Rex (1950a) gave a definition of blocking in terms of the shape of upper height fields, emphasizing the existence of an appreciable split flow into a double jet, a sharp transition from westerly to meridional flow and a persistence of the pattern. During the subsequent decades Rex's definition served as a model for developing other subjective methodologies (e.g. Sanders 1953; Austin 1980), while the ideas of Elliot and Smith (1949) did not find a successful continuity. From an historical perspective the early 1980s can be regarded as a turning point. The development of long and continuously updated data sets, and the widespread use of more powerful computers, promoted the design of machine-processed objective methods. The anomaly method was rescued by DG that identified blocking as isolated closed areas of Z500 anomalies exceeding a given threshold and lasting for a certain time. That same year, Rex's approach was pursuit by Lejenäs and Økland (1983) and later by TM, who adapted Rex's criteria into an objective method. They used the concept of zonal index that provides a measure of the westerly flow at each longitude from the Z500 meridional difference centred in a constant reference latitude. This index provides a local and instantaneous definition of blocking based on the detection of longitudes with easterly flows (the so-called blocked longitudes). TM also: (1) added a second gradient criterion to filter out other systems that marginally may fulfil the condition of easterly winds in the jet latitudes; (2) generalized the method to take into account the longitudinal extension and time duration of the block by demanding some persistence to a minimum number of consecutive blocked longitudes.

The TM and DG blocking definitions have suffered modifications through the years, mostly aimed to improve the characterization, structure and evolution of the blocked flow or to reduce the subjectivity and the number of required criteria to a minimum, but the essence of both blocking indices still persists and they are largely employed.

### 2.2 Assessment of blocking indices

A careful examination of advantages and shortcomings of the blocking indices is required to construct a methodology. The following discussion will focus on the two main blocking methods, based on the papers described in the previous section (Table 1).

TM is an efficient method that stands out by its simple applicability to large datasets. It provides a natural definition and avoids the problem of defining a proper climate mean state since it relies on the total field, but it suffers from the limitation of a longitudinal (i.e. 1-D) description of the block and the specification of empirical parameters such as the latitude at which the meridional gradient is computed and the predefinition of blocking sectors. On the other hand, DG provides a full 2-D (longitude–latitude) description of the block and a straightforward way of blocking identification, reducing the number of empirical parameters to a minimum. However, it requires time series long enough to derive a robust estimation of the mean field and the problem of a proper definition of the anomalies and thresholds has always been present since it involves some degree of arbitrariness.

A serious limitation of the TM index is its 1-D nature, which is unable to account for the extension, location and the spatio-temporal propagation of blocking events. As a consequence, methods based on this index are usually forced to pre-define preferred sectors where blockings can be found. This regional approach ensures blocking stationarity but simultaneously can miss blocks by transitions

**Table 1** Assessment of blocking detection indices

| Diagnosis | TM | DG | BGT |
|---|---|---|---|
| Pre-required parameters | Reference latitude | Anomaly definition | Reference latitude |
| | Blocking sectors | | Anomaly definition |
| Critical parameter | Reference latitude | Anomaly threshold | Reference latitude |
| | | | Anomaly threshold |
| Missed blocks | Immature and Ω-blocks | Not reported | Some doubtful Ω-blocks |
| Spurious systems | Cut-off lows | No blocking anomalies | A few ridge anomalies north of cut-off lows |
| Extension criterion | 1-D | 2-D[a] | 2-D |
| Tracking | No (eulerian) | Yes (lagrangian) | Yes (lagrangian) |
| Description of the block | 1-D | 2-D | 2-D |

Characteristics of blocking detection indices (*columns*) inferred from different estimators of the diagnosis quality (*rows*)

*TM* Tibaldi and Molteni (1990), *DG* Dole and Gordon (1983), *BGT* this work

[a] Not always demanded

between sectors. Moreover, the spatial scale of the block that is typically estimated from the 1-D extension of the reversal does not necessarily reflect the phenomenon's dimension. In fact, regional dipole-blocks are usually associated with easterly winds over areas much larger than those of omega blocks of comparable dimensions. Fortunately, some of these shortcomings have been partially overcome by refining the definition of regional blocking (Pelly and Hoskins 2003; Tyrlis and Hoskins 2008) or proposing 2-D expansions of the TM index that avoid a priori definitions of blocking sectors (Barriopedro et al. 2006; Diao et al. 2006; Scherrer et al. 2006).

Regarding the detection efficiency, the TM index can potentially lead to erroneous identifications since persistent cut-off lows that are anomalously displaced to the south can sporadically induce easterly winds. Recent modifications to the TM index have been attempted to avoid this shortcoming (e.g. Barriopedro et al. 2006; Diao et al. 2006). The method also presents limitations with atmospheric patterns that are difficult to catalogue from a meteorological point of view. They mostly refer to its generalised inability to detect omega blocks and its tendency to miss immature blocks (i.e. the early stages of block development). However, these caveats are often a conceptual problem that arises from the complexity of distinguishing blocks from open ridges rather than a weakness of the method itself. In that sense, the TM index identifies blocks as long as a closed anticyclonic circulation evolves. Otherwise, there are no easterly winds and the flow is catalogued as an open ridge. In other cases, however, omega blocks are filtered out with the TM index due to too demanding choices of the extension criterion that screen out omega blocks with small-scale reversals.

A deeper insight into blocking indices reveals that some of the limitations attributed to the TM index do not totally rely on the synoptic experience. The specification of the latitudes where a block can be found or the subsequent implication regarding the occurrence of just one blocking pattern per longitude is frequently regarded as a needless or even a serious limitation of the TM index. However, a thorough review demonstrates that this parameter cannot be ignored. The relationship between the jet stream and blocking was already recognized by Rossby (1939) and Namias (1950). Earlier studies based on visual blocking identification emphasized: (1) the weakening of the westerly flow as a straightforward feature of blocking occurrence and (2) the need of blocking search restricted to a latitudinal band representative of the westerlies in order to discern blocking from other type of structures such as subtropical and subpolar anticyclones (e.g. Treidl et al. 1981; Knox and Hay 1984). Depending on the method and the analyzed region, the lower latitudinal limit for blocking occurrence has been fixed in a range between 30°N (e.g. Treidl et al. 1981) and 50°N (Austin 1980), while the northern boundary seems to be of secondary importance and it has ranged between 65°N (Sanders 1953) and 80°N (Mullen 1989), sometimes imposed by the availability of data rather than by a stringent method's requirement. Thus, some consideration of the latitudinal occurrence of blocks should be made in objective procedures.

Another criticism to the TM index is the fact that the reference latitude is kept fixed through the whole NH (typically centred at 50°N). This assumption does not reflect realistically the spatial variability of the jet stream and hampers the applicability of the method to model simulations where the jet stream could be shifted as compared to the observed one by either a model bias (D'Andrea et al. 1998) or a climate change signal. This deficiency has recently been addressed by Pelly and Hoskins (2003), hereafter PH.

The need to adopt a reference latitude to properly place blocks was also stressed by Liu (1994) who compared the

objective criteria of DG with the subjective one of Rex (1950a) in order to investigate the conditions that positive anomalies must satisfy to be interpreted in terms of Rex blocking structures. He reported that blocking cannot be defined as an anomaly greater than some threshold value since the latitudinal position of the anomaly centre is also a critical parameter, with positive anomalies centred about 45° in the Euro-Atlantic sector usually representing northward extensions of subtropical anticyclones but not blocking of the westerlies. In addition to this, the DG index also suffers from a misleading interpretation of the total flow and a certain amount of arbitrariness on the choice of the threshold to catalogue blocks. Thus, while blockings are always associated with positive height anomalies, the reverse is not true and the occurrence of a persistent positive anomaly does not necessarily imply a blocking high (e.g. Charney et al. 1981). Thus, a variety of synoptic situations that do not perturb the westerly flow can be labelled as blocks from an anomaly based approach, including northward shifts of the jet, amplifications of subtropical or subpolar anticyclones or weak troughs. This caveat is the main limitation of examining anomalies rather than absolute flow, even when some studies have tried to minimize this effect by requiring severe anomaly thresholds (e.g. Sausen et al. 1995) or strict stationarity (e.g. DG).

## 3 The detection method

It is clear from the above discussion that a combined method of absolute and anomaly fields would be desirable since each approach emphasizes different but complementary relevant features of the same phenomenon. This section describes the method to build such a combined index. Relevant parameters involved in its definition will be catalogued as critical. Additional parameters required in the diagnosis (mostly aimed to account for the typical scales of blocking) will be referred to as secondary, since the results reported here changed little for variations in their thresholds. The purpose of this classification aims to deal with subjectivity in the choice of thresholds, as certain parameters do not allow the same level of arbitrariness than others. In any case, we must bear in mind that certain subjectivity is unavoidable when adjusting any parameter.

### 3.1 Data

Z500 is adopted as the base field in blocking detection for traditional reasons and intercomparison purposes. Daily Z500 fields and monthly zonal wind data at 500 hPa (U500) have been extracted from the NCEP-NCAR reanalysis (Kalnay et al. 1996) at 2.5°×2.5° resolution for the period 1950–1989 and the whole NH. As observational results will be compared to model simulations in Paper II, data have been interpolated to the same resolution of the model (ca. 3.75°×3.75°) so as to keep coherency throughout Paper I and II. Nevertheless, the same analyses performed at the original grid resolution did not change the results, supporting the relative independence of the detection method to grid resolution. The slightly awkward choice of the analysed period also corresponds to the present climate window available from the long-term model simulation (Paper II).

The computation of the anomaly field has been performed by removing the running annual mean and the seasonal cycle from the daily Z500 time series, $z(t)$, at each grid point, as described by Sausen et al. (1995), hereafter SKS (see Appendix). As the anomaly computation requires the estimation of the mean seasonal cycle (which may change with time), the procedure has been applied to time-windows of 25-years. Such a choice was found to reduce the computational expenditure and provide robust estimates of the mean seasonal cycle, although the specific window's width was not crucial for the subsequent analysis (not shown).

### 3.2 The daily detection index

From a combined perspective, blockings can be viewed as 2-D anomalies capable of reversing the absolute meridional height gradient. Figure 2 shows a schematic representation of the parameters used in the blocking index BI definition for a grid ($\lambda$, $\phi$) of ($ni$, $nj$) points and ($\delta\alpha$, $\delta\varphi$) longitude-latitude resolution. A novel index BI is designed from daily Z500 fields by detecting meridional jet-based reversals of latitudinal amplitude $\Delta\phi$ that are associated with 2-D positive Z500 anomalies north of a given reference latitude ($\phi_c$). A two-step approach is employed:

(i) *Detection of meridional height reversals*: instantaneous reversals at a given longitude can be identified from averaged (PH) or grid point-based (TM) field inversions. TM computed the meridional gradient using two $\Delta\phi$-equidistant grid points from a central latitude, $\phi_0$, while PH identified large-scale reversals as the difference of two $\Delta\phi$-averaged latitudinal belts north and south of $\phi_0$. TM increases the opportunities of blocking occurrence but it may produce spurious reversals as it does not take into account the large-scale signature of the block. Thus, the PH approach is adopted here, although there are little differences in the diagnosis performed by each index (not shown).

The index requires an estimate of the latitudinal scale of the block ($\Delta\phi$). Given that blocking episodes interrupt the passage of the transient mid-latitude weather systems, the latitudinal width of the synoptic activity in the storm tracks provides an indicative length scale of $\Delta\phi$ (PH). Although that quantity has traditionally been fixed to 10° by TM, PH found that 15° may reflect a more realistic approximation.

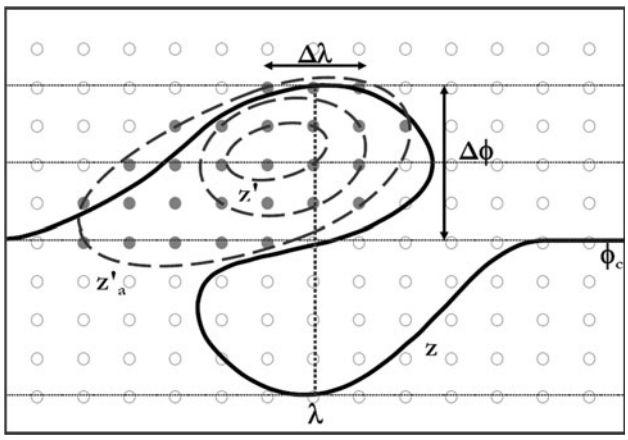


**Fig. 2** Construction of the blocking index. Schematic diagram of a block centred at $\lambda$. *Solid line* (*dashed lines*) is representative of the total (anomaly) height field $z$ ($z'$) during a blocking episode. *Dots* indicate the data grid. *Filled dots* reflect anomalies above a given threshold $z'_a$. $\phi_s$ ($\phi_c$) represents a characteristic latitude of high-synoptic activity (jet stream). Adapted from Knox and Hay (1984) and Pelly and Hoskins (2003)

As such, 15° has been chosen as a typical scale of $\Delta\phi$ in this study, the exact value was found not to be crucial, though. In order to account for some latitudinal variation of the block, $\phi_0$ is allowed to oscillate up to $\Delta\phi/2$ north and south of the reference latitude $\phi_c$. Thus, for each longitude and time step the meridional gradient is computed as follows:

$$ZI(i,\phi_0) = \frac{2}{\Delta\phi}\left[\sum_{j=\phi_0(i,m)}^{j=\phi_0(i,m)+\Delta\phi} z(i,j) - \sum_{j=\phi_0(i,m)-\Delta\phi}^{j=\phi_0(i,m)} z(i,j)\right]$$
$$1 \le i \le ni$$
$$\phi_c(i) - \Delta(m) \le \phi_0(i,m) \le \phi_c(i) + \Delta(m)$$
$$\Delta(m) = m\delta\varphi \quad 0 \le m < \Delta\phi/2\delta\varphi \qquad (1)$$

where the summed quantities are not area-weighted. The zonal index ZI identifies local and instantaneous meridional reversals when ZI is positive for any of the $\phi_0$ values. However, this approach may depend on the grid resolution, with coarser grids showing fewer opportunities for block occurrence. Thus, to avoid resolution biases, ZI is required to be positive over a given longitudinal interval $\Delta\lambda$ centred at each longitude $\lambda$. The mean zonal index $\overline{\mathrm{ZI}}$ is computed by averaging maximum ZI values (among those provided by $\phi_0$) for those longitudes within $\pm\Delta\lambda/2$:

$$\overline{\mathrm{ZI}}(i) = \frac{\delta\alpha}{\Delta\lambda+1}\left[\sum_{l=i-\Delta\lambda/2\delta\alpha}^{l=i+\Delta\lambda/2\delta\alpha} \mathrm{ZI}_{\max}(l,\phi_0)\right] > 0 \quad 1 \le i \le ni \qquad (2)$$

This modified index provides a measure of the mean zonal wind over a surrounding area regardless of the grid resolution, thus identifying regional and instantaneous blocking candidates. $\Delta\lambda$ is estimated as the deformation Rossby radius $L_R$ at typical block latitudes and can be considered as a minimum reversal 1-D extension for a circulation pattern to be considered a block (PH). That threshold is about 7.5° ($\Delta\phi/2$), which was also found sufficient to define a blocking pattern by Verdecchia et al. (1996). According to that, a given longitude is blocked if the mean zonal index $\overline{\mathrm{ZI}}$ is positive. In any case, differences between (1) and (2) are minor since most of the blocked longitudes raised by (1) often appear at successive grid points, the occurrence of isolated blocked longitudes being scarce and/or not persistent. Note that this blocking definition excludes the second gradient condition imposed by TM. Furthermore, the requirement of successive blocked longitudes in TM is here replaced by the demand of regional averaged conditions, thus increasing the opportunities for detecting omega blocks.

(ii) *Detection of 2-D height anomalies*: The next step of the detection process consists of extending the zonal detection to 2-D by identifying contiguous regions (i.e. clusters of grid points) where the anomaly field exceeds a threshold $z'_a$ around each blocked longitude (Fig. 2). A two-step procedure is applied: (1) the 1-D reversal is latitudinally expanded (Eq. 3) by searching along every blocked longitude grid points within a distance $\Delta\phi + \Delta\phi/2$ north of $\phi_c$ with anomalies exceeding $z'_a$ (blocked points); (2) in case of finding blocked points the 2-D blocking pattern is recognized by the surrounding grid points that exceed the anomaly threshold, so that the original blocked longitude is embedded in a new contiguous 2-D area (Eq. 4). Two grid points belong to the same contiguous area $r$ if they are adjacent or if a chain of grid points exceeding the anomaly threshold exists between them (SKS):

$$\overline{\mathrm{ZI}}_{2\mathrm{D}}(i,j) = \begin{cases} 1 & z'(i,j) \ge z'_a \quad \overline{\mathrm{ZI}}(i) \ge 0 \quad 1 \le i \le ni \quad \phi_c(i) \le \phi(j) \le \phi_c(i) + 3\Delta\phi/2 \\ 0 & \text{otherwise} \end{cases} \qquad (3)$$

$$\mathrm{BI}(i,j) = \begin{cases} r & z'(i,j) \ge z'_a \quad i,j \in \overline{\mathrm{ZI}}_{2\mathrm{D}} = 1 \quad 1 \le i \le ni \quad \phi_c(i) \le \phi(j) \le \phi(nj) \quad r = 1,2,\ldots \\ 0 & \text{otherwise} \end{cases} \qquad (4)$$

The algorithm also detects blocking action centres by computing the mass centre of the 2-D enclosed anomaly (Schwierz et al. 2004). Following the discussion in Sect. 2.2, this methodology just allows one blocking pattern per longitude unlike other anomaly based approaches that consider the occurrence of simultaneous anomaly signatures along the same longitude. This choice is based on the fact that two anomaly patterns placed along the same longitude cannot simultaneously reverse the jet stream.

### 3.3 Criteria

Two critical parameters must be computed before applying the blocking index: the reference latitude, $\phi_c$, and the anomaly threshold $z'_a$.

#### *3.3.1 Reference latitude*

The reference latitude $\phi_c$ can be inferred from either the location of the jet stream or the regions of maximum mid-latitude weather system activity since blocking is associated with both the suppression of the former and the interruption of the latter. TM adopted the first approach and assumed a longitudinally constant time-invariant jet stream at 50°N, whereas PH used the second concept by computing the latitudinal maximum of the climatological annual mean high-pass transient eddy kinetic energy at 300 hPa.

Here, $\phi_c$ has been estimated at each longitude as the latitudinal maximum of 5-day high-pass filtered Z500 variance, which has been weighted by the cosine of the latitude to account for the change of area with latitude and to avoid any effect of the specific grid employed in its computation. The choice of 5 days is a typical threshold for minimum blocking duration and retains most of the synoptic variability. $\phi_c$ values are derived for every month and year by defining a two-folded running window of: (1) 90-day centred in the given month and (2) 25-year centred in the given year. That provides $90 \times 25$ points of high-pass Z500 daily field per month and year to compute the high-pass filtered Z500 variance. Reference latitudes at successive longitudes are only allowed to oscillate $\Delta\phi/2$ north and south relative to that of the previous longitude to avoid abrupt transitions.

The 3-month window takes into account seasonal changes in transient eddy location and simultaneously allows a smooth transition in $\phi_c$ from month to month. The seasonal approach is preferred to the annual one because annual-fixed values may include subtropical anticyclones as blocks during periods of northward eddy migration. Furthermore, a given model may suffer from an excessive seasonality in the location of synoptic activity. Long-term variations in $\phi_c$ are also considered by the 25-year window so as to account for meridional shifts that may have occurred in the past and might occur also under a climate change scenario. The width of 25-year was chosen, after testing several longer and shorter window sizes, as a compromise between long periods (that provide robust estimations) and short periods (that reflect higher-frequency variations).

Figure 3 displays two examples of $\phi_c$ and the associated zonal wind obtained for mid-winter and mid-summer conditions. $\phi_c$ captures regions of maximum synoptic activity, which lie north of the main zonal wind belt at extratropical latitudes. Thus, $\phi_c$ can be regarded as the preferred central latitude for blocking occurrence, whereas the jet stream lies at latitudes where a block exerts a major impact in the zonal wind (i.e. its equatorial side). Due to the overall good correspondence between them and for the sake's of simplicity, the terms reference latitude and jet stream will be used indistinctly from now on, keeping in mind that they are not the same in a rigorous sense.

Figure 4a shows the mean reference latitudes, $\phi_c$, for two seasons and the whole period. Regional and seasonal variability is consistent with poleward (equatorward) jet latitudes over the Atlantic (Pacific) and a generalized northward shift in summer. Most of the variability in the reference latitude is explained by monthly-to-seasonal (light shading) rather than interannual (dark shading) variability. The largest departures from the annual mean spread along the Pacific, supporting that an approach based on annual reference latitudes might not capture interseasonal blocking variability.

#### *3.3.2 The anomaly threshold*

There is no agreement in the minimum threshold that anomaly patterns must meet to be considered as blocks. Different subjective values have been adopted, ranging from 100 gpm (e.g. Carrera et al. 2004) to 300 gpm (SKS). Other authors have attempted objective definitions (DG; Charney et al. 1981) or seasonal dependent thresholds (Shukla and Mo 1983; Knox and Hay 1984).

Here, following DG, the anomaly threshold is computed as the one standard deviation level of the daily anomaly distribution obtained for those grid points lying north of the reference latitude. To account for seasonal variability, the anomaly threshold is derived for every month from the 3-month anomaly distribution centred in the given month. Figure 4b shows the annual and two seasonal mean distributions, corresponding to winter and summer months. The distributions reveal a Gaussian shape and anomaly thresholds ranging from 135 gpm in winter to 95 gpm in summer. On allowing seasonal changes in the anomaly threshold, we assume that blocking significantly contributes to the intraseasonal, but not so much to the

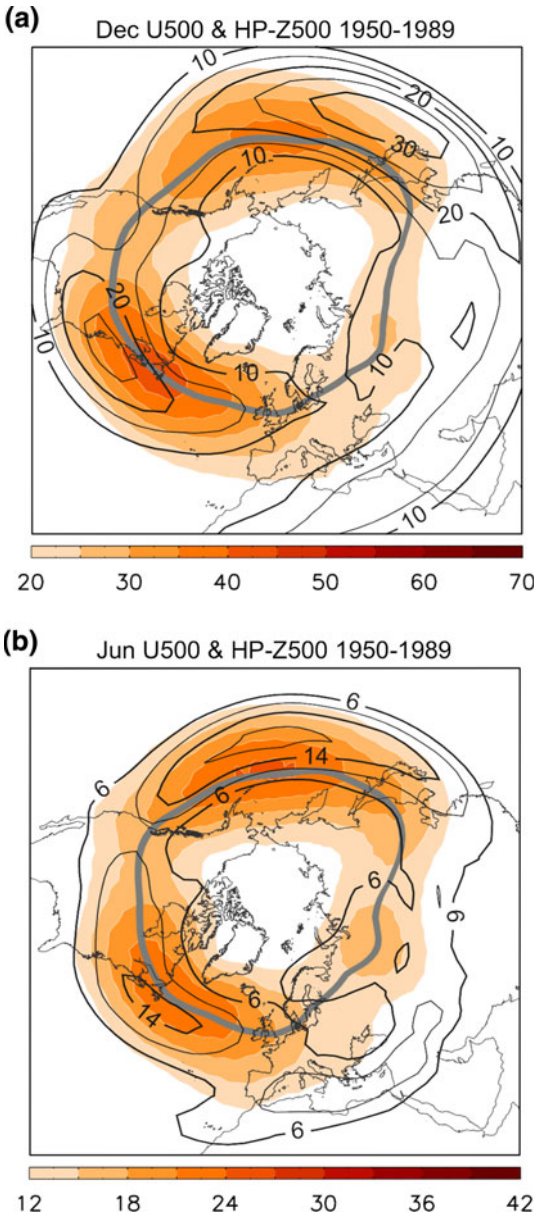


**Fig. 3** The reference latitude. Long-term (1950–1989) mean reference latitude (*thick solid line*, $\phi_c$) for: **a** January; **b** July. *Shaded areas* (*solid lines*) show the long-term standard deviation of the 5-day high-pass filtered Z500 field in gpm (zonal wind in m $s^{-1}$) for the 3-month period centred in that month. Note the difference in the scale

interseasonal variability. However, unlike the reference latitude, monthly anomaly thresholds have been kept fixed through the whole period of analysis, so that changes in variability at interannual and longer time scales will arise as fluctuations in blocking frequency. These assumptions are made on the basis that a large amount of interannual variability can result from intraseasonal processes (e.g. Schwierz et al. 2006). In particular, blocking can play an important role in modulating the interannual variability patterns, especially over the Euro-Atlantic sector (e.g. Croci-Maspoli et al. 2007).

As the anomaly criterion is not absent of certain arbitrariness, a test was performed to verify if the adopted threshold was in agreement with the amplitude of the anomalies observed during cases of meridional Z500 reversals across the reference latitude. The annual composite of the latitudinal Z500 anomalies for those days and longitudes when the zonal wind around the reference latitude was reversed reveals a north–south anomaly dipole with local maximum values of about 150 gpm north of the reference latitude (Fig. 4c). Assuming a latitudinal amplitude of $\Delta\phi \sim 15°$ for blocking patterns, a minimum anomaly base value of 125 gpm is obtained, which is close to the annual average (115 gpm) of the monthly anomaly thresholds adopted here. Similar values are also inferred from the maximum of the band-pass Z500 deviation (not shown) and from objective (Charney et al. 1981) or empirical (Knox and Hay 1984) approaches.

### 3.4 Additional criteria

The daily blocking index has to be supplemented by further conditions reflecting the spatial extension and time duration that distinguish a blocking episode from transient (not-persistent) systems. Most of these criteria were found to be secondary. As a consequence, some arbitrariness can be adopted in their definition.

#### *3.4.1 Extension*

According to TM a large-scale blocking occurs if a given number of consecutive longitudes are found at a specific instant in time. Unlike TM methodologies, a 1-D extension criterion is not demanded here, one isolated longitude being enough to catalogue a blocking candidate. This choice is based on the fact that: (1) the mean zonal index (Eq. 2) already accounts for some longitudinal extension of the block; (2) there is no straightforward way of estimating the 2-D spatial scale of the block from the extension of the reversal. As a consequence, the blocking extension is here determined from the 2-D area delimited by the anomaly threshold. A characteristic blocking scale of the order of 1–2 $\times$ $10^6$ $km^2$ is estimated by assuming standard values of $L_R \sim 7.5°$ as a minimum longitudinal scale (e.g. Verdecchia et al. 1996; PH) and $\Delta\phi \sim 15°$ as a typical latitudinal scale of the block (e.g. PH). Thus, 2 $\times$ $10^6$ $km^2$ has been imposed as a minimum extension criterion to the daily 2-D blocking anomalies.

#### *3.4.2 Tracking*

The specification of persistence requires a tracking algorithm that identifies blocking episodes as successive daily blocks with varying extension and location. In this study,

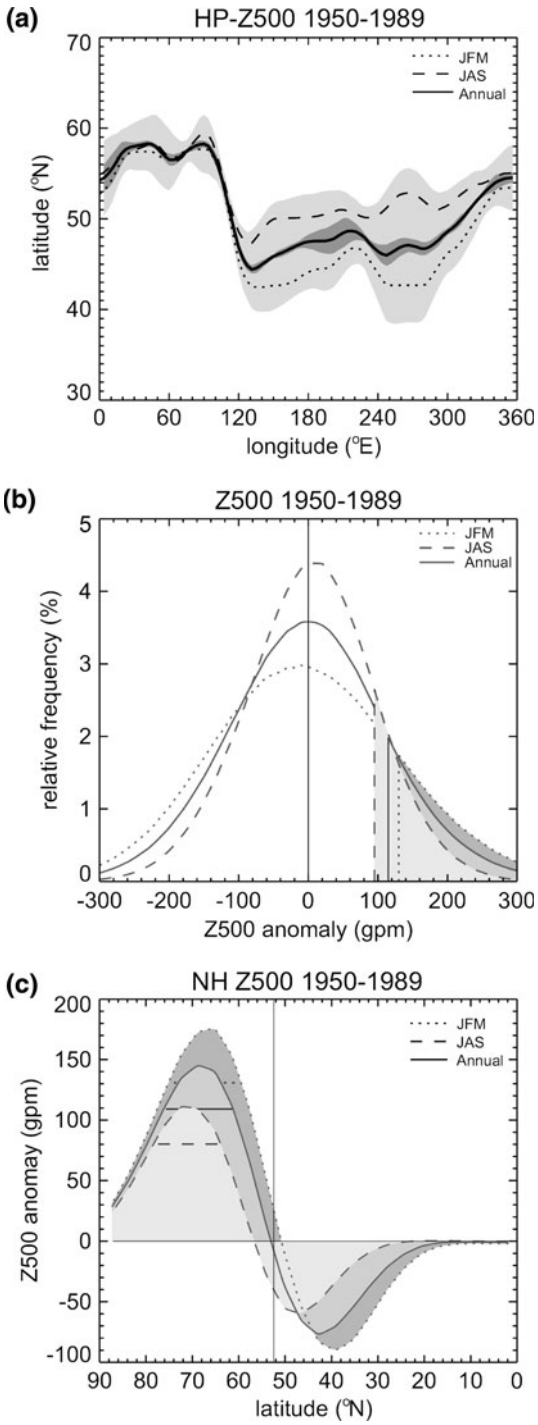


**Fig. 4** Determination of critical parameters. **a** Longitudinal distribution of the 1950–1989 annual averaged reference latitude ($\phi_c$, *solid line*). *Light* (*dark*) *shaded areas* indicate the $\pm 2\sigma$ level of the monthly (annual mean) time series; **b** annual frequency distribution histogram of daily Z500 anomalies for the period 1950–1989 and all grid points north of the reference latitude $\phi_c$ (*solid line*). The anomaly threshold, $z'_a$, is displayed as the $1\sigma$ level of the distribution; **c** annual composite of daily latitudinal cross-section Z500 anomalies for meridional height reversals across the reference latitude at any longitude of the NH (*solid line*). The latitudinal range $\Delta\phi$ centred on the local maximum is marked as anomaly baseline. *Vertical solid line* denotes the averaged reference latitude $\phi_c$. *Dashed* (*dotted*) *lines* in **a**, **b** and **c** represent the corresponding distributions for July–August–September (January–February–March)

the spatial coherence is considered by requiring a specified percentage of area-overlap between two blocking candidates detected in successive time steps (e.g. Schwierz et al. 2004). Thus, a given block detected at a certain day $d_i$ is said to persist on the following day $d_{i+1}$ if the $d_i$ blocked area overlaps with a $d_{i+1}$ block by a minimum amount. If more than one block on day $d_{i+1}$ verifies this condition, that presenting the highest overlapping is chosen as the next position of the block of the day $d_i$. The requirement of a minimum overlapping indirectly imposes a limit to the speed of the block, but it also allows simultaneously for a reasonable movement.

Available literature discloses maximum speeds ranging between 5° day$^{-1}$ (Metz 1986) and 20° day$^{-1}$ (Hartmann and Ghan 1980). Several studies have suggested that an upper speed limit for blocking movement can be set at the characteristic velocity of travelling large-scale disturbances, which is of the order of 10°–15° a day (e.g. Treidl et al. 1981). Thus, assuming a typical longitudinal scale of about $L_R \sim 15°$ and a maximum displacement below 10° day$^{-1}$, a simplified analysis suggests minimum overlapping estimates of about 50% (not shown), which has been chosen here as minimum percentage of area-overlap between successive daily blocks.

### 3.4.3 Duration

Minimum duration criteria of individual blocking events found in the literature cover the whole range of temporal lengths between 1 (Lejenäs and Økland 1983) and 10 (Rex 1950a; Kaas and Branstator 1993) days. Although the specific threshold is not too critical for the method, an objective criterion would be desirable by virtue of the wide spectrum of values employed in the literature.

It is frequently argued that the exponential shape of the blocking duration distribution is a common and unique feature of blocking patterns (e.g. DG, PH). When the cumulative histogram (i.e. the number of blocking episodes with durations equal or higher than a given bin) is plotted in a semilog-plot, the deceasing exponential curve appears linear, the slope of the linear regression being interpreted as a characteristic temporal scale of blocking. This reasoning has been usually employed to stress that responsible mechanisms of blocking formation and maintenance tend to follow the distribution of a Markovian process (i.e. the occurrence probability of a blocking event of $t$ or more

days is independent of $t$), although a more recent study has confirmed that blocking is not totally consistent with such a process, especially for long-lasting episodes (Masato et al. 2009). This rationale is used here to establish an objective duration criterion. In order to obtain the duration distribution, a range of durations has been set, with the lower limit fixed to 4 days (as a commitment between a long enough threshold above the synoptic scale to observe significant impacts, and a short one to have a representative sample) and the upper one to 15 days (to avoid dispersion and lack of robustness in the tail of the distribution). Figure 5a shows the well-known exponential distribution of blocking persistence. The linear slope in the log-plot (Fig. 5b) provides the minimum duration criterion $t_0$, which is found to be roughly 4 days.

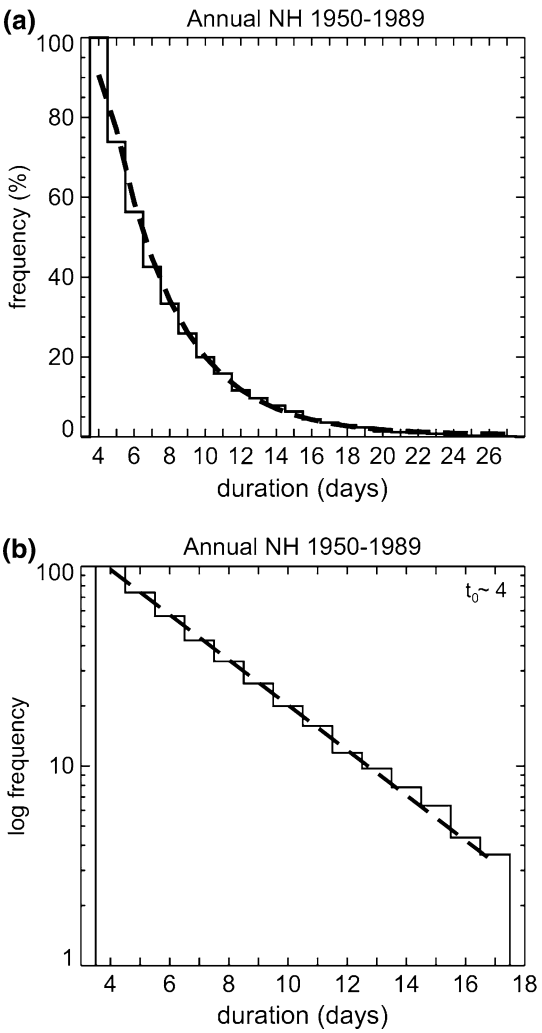


**Fig. 5** Duration criterion. **a** Normalized distribution of blocking events with durations equal or higher than the given bin. The number of blocking episodes of a given bin is normalized by the total number of events. The *dashed line* indicates an exponential fit; **b** as **a** but in a semilogarithmic-scale plot. The nearest integer value ($t_0$) to the slope in the linear regression (*dashed line*) is adopted as the minimum duration criterion

### 3.5 Efficiency of the method

This method shares some of the advantages of the TM and DG indices (see Table 1). A 2-D representation of blocking is possible by virtue of the anomaly based approach, while the method still preserves the computational-time efficiency, since only those longitudes with meridional reversals are examined as blocking candidates (and not the full 2-D field). Aside from that, the method is fully applicable to model simulations since critical thresholds are not pre-defined but specific of the data set employed.

On the negative side, the number of critical parameters required in the identification of blocking is higher than just using one approach, and so, instead of needing only a reference latitude or an anomaly threshold, both are now required. Nevertheless, as stated before, a reference latitude is usually an unavoidable parameter in blocking identification. On the other hand, the inclusion of an anomaly based criterion is automatically balanced with the exclusion of other artificial empirical parameters that would otherwise be required, such as the a priori definition of blocking sectors, the need of estimating block's dimension from the extension of the reversal or the lack of coherency in identifying individual blocking propagation from 1-D descriptions. Thus, the increment of specifications required to apply the proposed method is expected to be compensated by the improvement in blocking diagnosis.

Figure 6a shows an example of potential misleading blocking detection relative to the 21 January 1950. The method described here identifies two blocking candidates over the Euro-Atlantic and Pacific sectors with standard blocking signatures. On the other hand, the deep cut-off low over Eurasia generates easterly winds over typical latitudes of the jet and would be wrongly detected as a block by the zonal index (as realized by non-null values of $\overline{ZI}$). Simultaneously, the positive height anomaly lying over North America reflects an anomalous shift of the jet in the total flow and would be included as a block in the DG method when, in fact, there is no weakening of the westerlies. None of these two systems are catalogued as blocks with our method since the requirement of an anomaly threshold overcomes the problem of identifying deep cut-off lows as blocks, while the reversal criterion in the absolute field ensures that the so-detected anomaly signatures are in fact blocking the westerlies. Figure 6b shows another example of potential misleading blocking detection when blocking patterns are just detected from height anomaly based blocking indices. Here, the DG index has been computed after applying the algorithm described in previous sections but without demanding the presence of

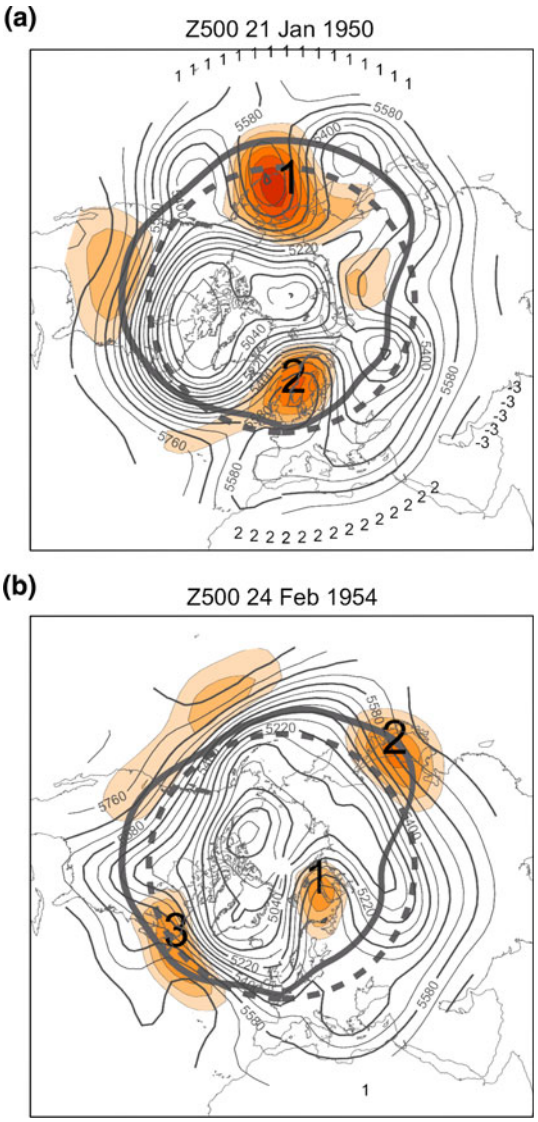


**Fig. 6** Blocking detection. Two examples of blocking patterns identified from: **a** the proposed blocking index; **b** an anomaly based blocking index (after DG). *Solid lines* indicate the Z500 daily field (CI 50 gpm). The reference latitude, $\phi_c$, for the given month and year and the TM central latitude, 50°N, are displayed in *grey thick solid* and *dashed lines*, respectively. *Shaded areas* show positive anomalies with contour interval of 50 gpm, starting at 115 gpm. Longitudes along 25°N with positive (negative) values reflect local reversals that are (not) associated with anomalies above $z'_a$. Blocking mass centres are successively labelled with the same number assigned to their blocked longitudes

meridional height reversals in the absolute flow. This modified version of the DG index identifies several blocking candidates when only one of them (over Eurasia) shows typical blocking signatures. In this case, the absolute flow blocking condition allows screening out positive anomalies that are not attributable to blocks.

These two examples support that the method presented here succeeds in identifying persistent anomalies hidden by the mean field but associated to a specific weather regime in the total flow. Nevertheless, we acknowledge that a few examples are insufficient to guarantee an improved detection. Such an accomplishment requires a lengthier and thorough comparison of results obtained with the method presented here and those attained by different approaches. That exercise is performed in Sect. 4.2.

## 4 Climatologies

In this section blocking activity will be assessed from both a grid-point description and an event-based approach. For the sake of brevity, the description will focus on overall NH features and specific blocking sector signatures will not be addressed.

### 4.1 Observed features

The resulting 2-D geographical distribution of blocking frequency is displayed in Fig. 7a. It has been computed as the ratio of the number of days when a grid point showed a blocking anomaly to the total number of days of the year. Two main sectors of blocking activity are observed over the eastern Atlantic and Pacific, in good agreement with the coincidental regions of maximum band-pass-filtered variability and wave amplification (figures not shown). The Atlantic centre is much broader than its Pacific counterpart and extends well into Eurasia. Euro-Atlantic blocks are also more frequent, almost doubling the occurrence of Pacific blocks.

Figure 8a shows the annual mean blocking frequency as a function of the longitude (i.e. the 1-D distribution of blocks) estimated as the percentage of days of the year when a given longitude was blocked. Again, the distribution is dominated by two maxima over the western Euro-Atlantic region and eastern Pacific as well as a weaker secondary maximum over Eurasia. Some studies have pointed out this region downstream of the Ural Mountains as a third preferred region for blocking occurrence, associated with the Mediterranean storm track (Lupo and Smith 1995; Wang et al. 2009). This action centre is better discernible from the Euro-Atlantic one in seasonal distributions (not shown). The bottom plot of Fig. 8a shows a longitude-time Hovmöller diagram displaying the monthly frequency of blocking days (in percentage). Although there are changes in the seasonal distribution of blocked days and in the longitude showing the maximum values, the dominant blocking sectors are appreciable through the whole year, appearing in late autumn, peaking in winter and decaying in spring. These results compare well with observational climatologies (e.g. Rex 1950b; Treidl et al. 1981).

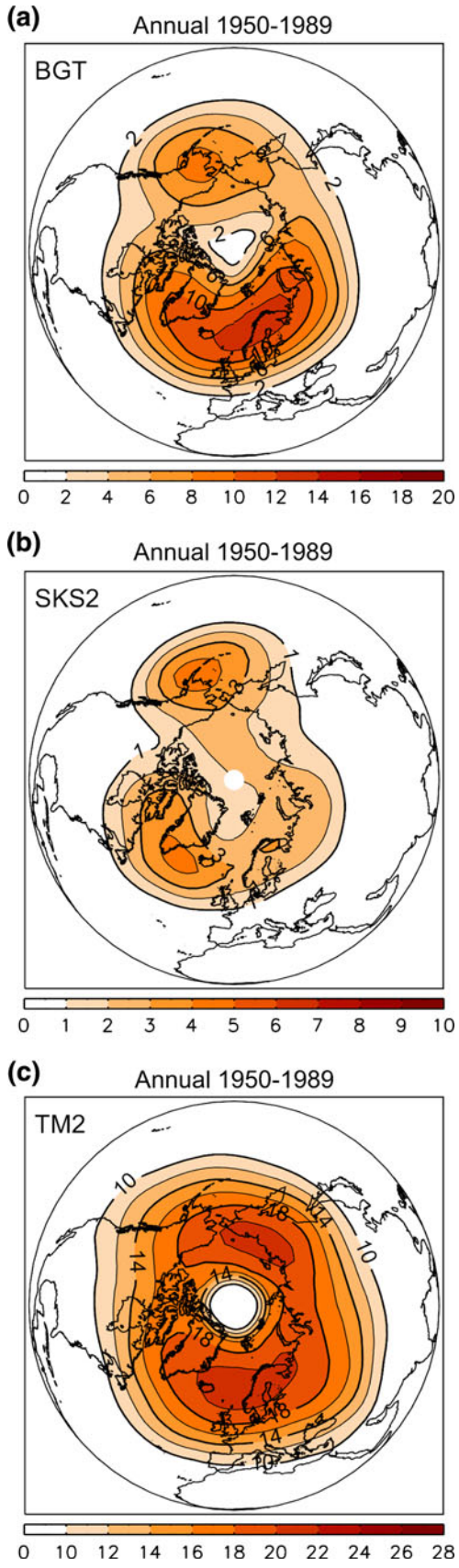


◄ **Fig. 7** 2-D blocking distribution. Climatological annual mean blocking frequency (in percentage of annual days) as derived from **a** the proposed index (*BGT*) and a modified version of: **b** the SKS index (*SKS2*); **c** the TM index (*TM2*). See text for details

In what concerns the statistical description of individual blocking events, this approach provides an alternative way of describing blocking activity by computing monthly time series of blocked days (i.e. number of days when a blocking episode was detected anywhere), blocking events and average durations (Fig. 9). Blocking activity reflects strong seasonal variability with maximum occurrences in late winter and early spring and minimum frequencies in late summer and early autumn. Similar annual cycles are gleaned for blocking events (Fig. 9b). However, the distribution of blocked days reaches its peak earlier in the year than that of blocking events due to the longer persistence of winter blocks (Fig. 9c, e.g. Wiedenmann et al. 2002; Diao et al. 2006).

These seasonal features have already been noted in previous studies based on TM index descriptions (e.g. Tibaldi et al. 1994; Barriopedro et al. 2006). On the other hand, anomaly based methodologies, which do not usually make use of event descriptors, tend to place the maximum of blocking activity in winter (e.g. DG; Shukla and Mo 1983; SKS). This discrepancy has been partially attributed to the different nature of the blocking indices employed. However, it should be noted that maximum blocking activity in our method is also confined to winter if a 2-D grid-point approach is employed (not shown). As a consequence, differences could also be explained by the methodology adopted to estimate blocking activity. Thus, an indicator based on the number of blocked days does not take into account the simultaneous occurrence of blocking episodes, which is more prone to occur in winter (Lejenäs and Økland 1983). On the other hand, grid-point estimates depend on the extension of the blocks, whose averaged sizes peak up in winter (e.g. Wiedenmann et al. 2002; Diao et al. 2006). As a consequence, while blocked days statistics (typical of TM-based methodologies) tend to underestimate winter blocking occurrence, grid-point blocking estimates (largely employed in anomaly based blocking methods) tend to overestimate it, producing the visual impression of spring maxima in the former and winter maxima in the latter.

### 4.2 Comparison with previous indices

To evaluate the new index proposed here (BGT hereafter) a comparison with a set of standard absolute- and anomaly based blocking indices employing both 1-D and 2-D

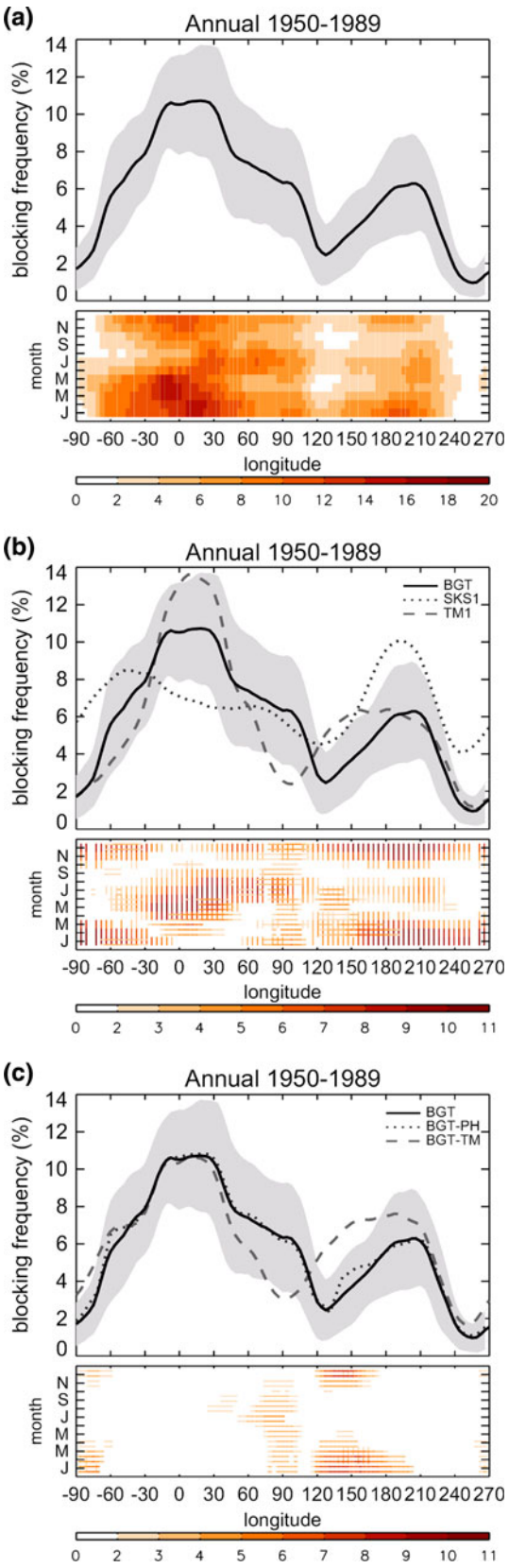


◀ **Fig. 8** 1-D blocking distribution. Annual mean frequency of blocked days (in percentage to the total days) as a function of the longitude (*solid lines* in **a**, **b**, **c**). *Shaded areas* denote the $\pm 1\sigma$ level of the mean distribution. *Dashed/dotted lines* indicate the corresponding climatology after employing: **b** the TM1 index/the SKS1 index; **c** space–time fixed reference latitudes at 50°N (*BGT-TM*)/time-invariant reference latitudes (*BGT-PH*). The bottom graphics display **a** the longitude-time Hovmöller diagram of monthly blocking frequency (in percentage of its number of days) and its difference with: **b** TM1/SKS1; **c** BGT-TM/BGT-PH in *horizontal/vertical lines*. Negative differences are shown in absolute value. Only differences exceeding 2% in absolute value and significant at $p < 0.1$ after a two-tailed Student's $t$ test are shown in the *bottom panel* of **b** and **c**. See text for details

approaches has been performed. They include: (1) the TM-based index employed by Barriopedro et al. 2006 (TM1 hereafter); (2) a 2-D version of the TM index (TM2 hereafter) formulated according to the same methodology described in this study but employing a constant reference latitude fixed at 50°N, a 1-D minimum extension criterion of $\Delta\phi$ (15°) and $z'_a = 0$ gpm so as to minimize the anomaly field influence in the index performance and keep criteria as close as possible to the original TM index; (3) the SKS index, but with slightly different anomaly thresholds (SKS2 hereafter). SKS2 blocks are identified as adjacent grid-points in the 3-D longitude-latitude-time domain with anomalies exceeding a certain threshold $z'_{a1}$. The so-detected areas are then contiguously extended to those points where the anomaly exceeds a second threshold $z'_{a2}$ ($z'_{a1} > z'_{a2}$). SKS set the specific parameters in $z'_{a1} =$ 300 gpm and $z'_{a2} = 250$ gpm. Here, these reference values have been fixed to the $2.5\sigma$ (285 gpm) and $2\sigma$ (230 gpm) levels of the annual anomaly height distribution of Fig. 4b, respectively, in order to raise some objectivity in the choice of margins; (4) a 1-D reduction of the SKS index (SKS1 hereafter) obtained by counting as blocked those longitudes where a SKS2 blocking pattern was detected at any grid point (one or more) along its meridian (SKS). For all blocking approaches a persistence of 4 days is required.

Some dissimilarity between BGT and the standard blocking indices SKS1 and SKS2 is expected due to methodological differences, namely the removal of the meridional height inversion condition and the anomaly threshold. Further differences are expected because SKS2 (and hence SKS1) allows: (1) overlaps and sizes of any magnitude; (2) blocks at any grid point of the NH; (3) no seasonal variation of the anomaly threshold. On the other hand, the change of the reference latitude and the relaxation of the anomaly threshold in TM1 and TM2 are the main sources of discrepancy with BGT.

The distribution pattern of SKS2 blocks (Fig. 7b) shows the well-known twofold dominant structure of this kind of

methods, with preferred regions for blocking occurrence confined to areas of maximum Z500 variance, whereas the TM2 block distribution (Fig. 7c) tends to emphasise regions of maximum wave amplification, specially over the Atlantic. Obviating the expected differences in the reported blocking frequency (the same block is counted at different grid-points depending on the anomaly threshold adopted for each index), there are two noteworthy features of the SKS2 index in disagreement with BGT: (1) Pacific blocks are relatively more frequent than the Euro-Atlantic counterparts; (2) Euro-Atlantic blocks are confined to its western margin. As compared to BGT, the TM2 index: (1) yields a broader Pacific maximum and a higher frequency rate of Pacific versus Euro-Atlantic blocks; (2) emphasizes western Pacific as a secondary region of block activity. These discrepancies are also inferred from Fig. 8b, which shows the zonal blocking distribution derived from BGT (solid line) and the 1-D blocking indices, TM1 (dashed line) and SKS1 (dotted line).

None of the features missed by BGT and identified by SKS2 or TM2 and their respective 1-D versions seem to compare well with the synoptic experience. Subjective and objective studies have identified a more active Atlantic sector (e.g. Rex 1950b; Treidl et al. 1981) with higher blocking frequencies over its eastern side (e.g. Kaas and Branstator 1993; Wiedenmann et al. 2002). On the other hand, blocking activity highlighted by the SKS2 index over western Atlantic or by the TM2 index over western Pacific is not in agreement with preferred locations of a climatological trough and an intense jet stream. In particular, the TM signature over the western Pacific has been explained in terms of the inappropriate choice of spatially constant reference latitudes at 50°N (PH), which is suitable for the Atlantic sector, but too far north from the actual location of the Pacific jet (Fig. 4a).

Some of the above reported features are comparable to those described by Doblas-Reyes et al. (2002) and Scherrer et al. (2006) who assessed performance differences between TM and SKS indices. To explain some of these discrepancies, several explanations have been proposed: (1) the enhanced detection of different types of blocking by each individual index, with dipolar blocks, more common in the Euro-Atlantic sector, being easily diagnosed with the TM index and omega-type blocks, characteristic of the Pacific sector, being better captured by the SKS index; (2) the influence of the time-mean structure, with open ridges and weaker-than-normal troughs (typical of western ocean basins) being interpreted as blocks by SKS; (3) the blocking stages that each index highlights, anomaly based indices being activated in the early stages of block development as northerly jet stream deviations over the western

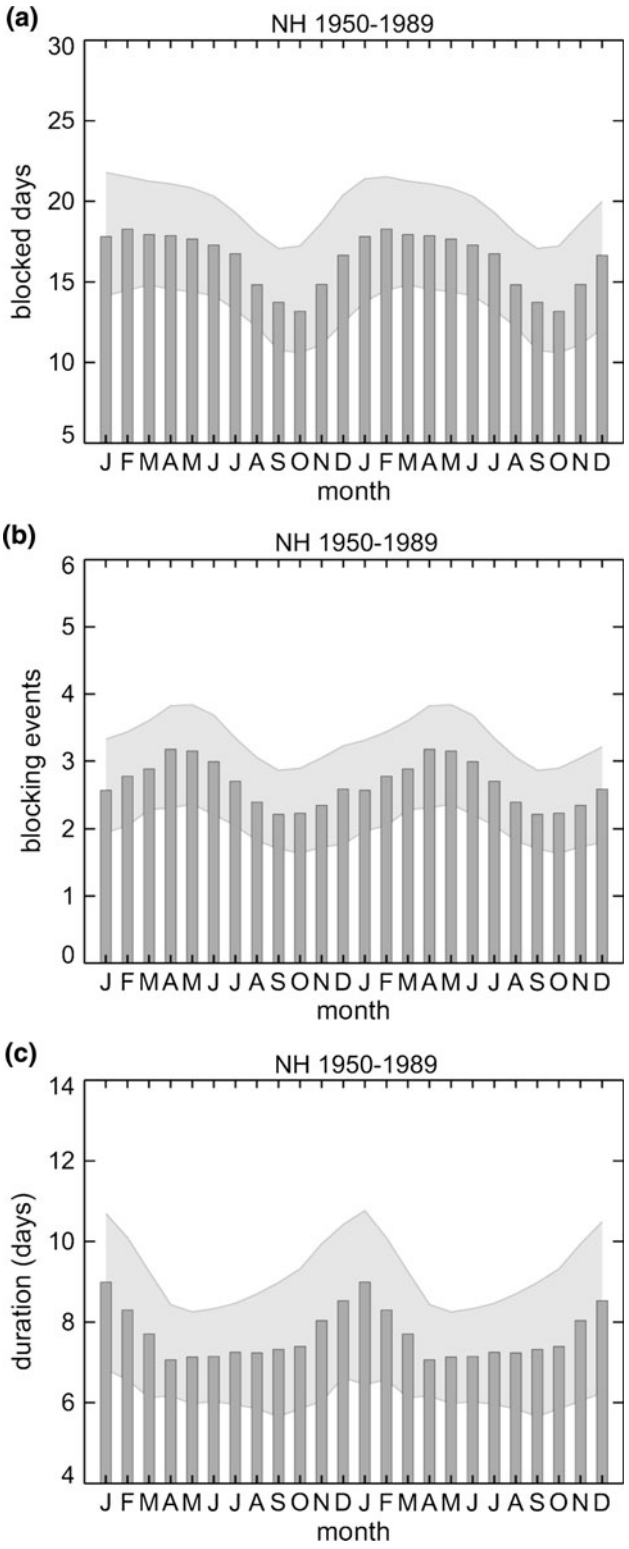


**Fig. 9** Blocking event characteristic parameters. Long-term annual cycle of Northern Hemisphere: **a** blocked days; **b** blocking events; **c** blocking duration (*days*). Two annual cycles are shown for better visualization. *Shaded areas* indicate the smoothed $\pm 0.5\sigma$ level

basins of both oceans and absolute-based descriptors being more likely to diagnose the mature stage of the block, when the quasi-closed anticyclonic circulation is well established over the eastern side of both oceans. Therefore, discrepancies in the climatologies reported by the TM and SKS indices are partially caused by the fundamentally different concepts behind their definitions, which highlight the regions with maximum Z500 wave amplification and Z500 variance, respectively. In that sense, BGT index provides a satisfactory compromise, respecting both the maxima of intraseasonal band-pass variance and the climatological regions of wave amplification.

In order to further stress the cause of these differences, blocking signatures detected by one index and missed by another have been computed over four sectors (Fig. 10): western Atlantic (WAT; [285, 345]°E), eastern Atlantic (EAT; [345, 45]°E), western Pacific (WPA; [120, 180]°E) and eastern Pacific (EPA; [180, 240]°E). A given sector is said to be blocked one certain day if the daily centre of a blocking episode falls within that sector. To avoid seasonal biases in the composites of the absolute flow, the analysis has been confined to January–February–March (JFM). The key regions are the Euro-Atlantic sector for SKS2 and the Pacific sector for TM2, which, respectively, concentrate maximum frequency differences with BGT (bottom plot of Fig. 8b).

The composite for the blocks detected by BGT and missed by the SKS2 over EAT is shown in Fig. 10a while Fig. 10c illustrates the corresponding composite for blocks missed by the TM2 index over EPA. Both figures reflect a standard blocking signature with wave amplification north of the jet stream associated to regionally localized positive height anomalies. The EAT pattern is relatively weak because of the removal of very intense blocking anomalies counted by both BGT and SKS2. WAT block regimes detected by SKS2 and missed by BGT (Fig. 10b) reveal positive anomalies extending over a climatological region of deep troughs and strong westerlies. However, there is no clear meridional displacement signature in the absolute field, suggesting that, apart from blocks, other weather systems with no interruption of the westerlies are identified by the SKS2 index. Among them, it is worth mentioning subpolar Greenland anticyclones and Atlantic open ridges, which are not considered blocks in statistical multivariate methods of weather regimes classification (e.g. Vautard 1990; Michelangeli et al. 1995). From the BGT point of view, a persistent positive anomaly does not necessarily imply the existence of a blocking high, and hence, none of these systems could easily fulfil our criteria. Further analyses have also been performed to identify blocks that would result after applying our methodology but without demanding the presence of meridional height reversals in the total flow. Results reveal maximum departures with BGT in the western margins of both oceans, where near 50% of persistent anomalies above the prescribed threshold $z'_a$ do not actually imply interruptions of the jet stream (not shown).

The signatures of WPA blocks detected by TM2 and not present in BGT display an amplified ridge with height reversals over north-eastern Siberia (Fig. 10d). However, pressure minima (instead of amplified waves) evolve north of the jet stream and positive anomalies are weak and too far north of the jet stream so as to have an effect in the propagation of transient systems and the intensity of the westerlies. From the anomaly absolute combined perspective of BGT, the existence of a height reversal does not necessarily denote a blocking high.

To assess the solely effect of the reference latitude, blocking output was examined (Fig. 8c) after employing time-invariant reference latitudes based on either spatially fixed values at 50°N (dashed line) or the annual mean of $\phi_c$ (dotted line), as in TM and PH, respectively. Maximum monthly blocking frequency departures in the TM-based approach of our blocking index occur in regions where the jet stream significantly deviates from 50°N (bottom plot of Fig. 8c). The TM underestimation over Eurasia results from reference latitudes being placed too far south of the actual jet stream. The opposite occurs over western Pacific. Differences are sustained in Eurasia through the whole year because of the relatively low intra-annual variability of the jet over there (Fig. 4a). In western Pacific, differences are mostly confined to winter, when the intensity of the jet stream increases and moves farther south of TM latitudes, thus increasing the probability of detecting easterly winds in the TM-based approach. When reference latitudes are allowed to vary in space but not in time (PH-based approach of our index) differences decrease considerably, almost suppressing the bias introduced by the TM latitudes. However, discrepancies are still observed in seasons and regions where the jet stream intensifies and deviates from its annual mean position (e.g. western margins of both oceans in winter). These results suggest that an approach based on annual time-fixed reference latitudes provides a realistic approximation, but it could not be the case in the surrogate climate of a model.

## 5 Conclusions

An updated review of previous blocking detection methods has been provided herein, assessing the main shortcomings and advantages of two widely employed standard indices. Results from these blocking indices suggest that an improved diagnosis should be performed without ignoring both the absolute and the anomaly fields. In fact, some caveats and limitations associated to traditional blocking indices can be partially overcome by merging them in a single blocking indicator. A new combined index that

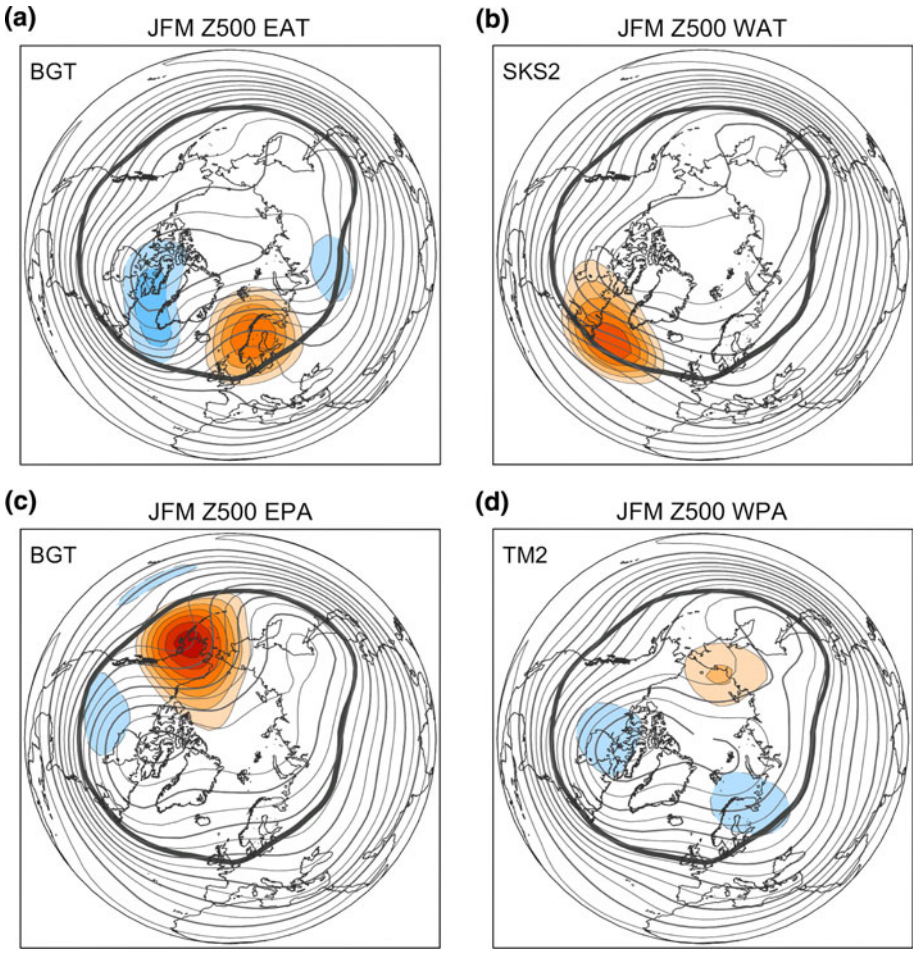


**Fig. 10** Regional blocking signatures. Composites of Z500 (*solid lines*) and Z500 anomalies (*shaded areas*) for winter blocked days: **a**, **c** detected by BGT and missed by **a** SKS2 in EAT, **c** TM2 in EPA; **b** detected by SKS2 and missed by BGT in WAT; **d** detected by TM2 and missed by BGT in WPA. *Red* (*blue*) *shaded areas* contoured by *solid* (*dashed*) *lines* indicate positive (negative) anomalies with contour interval of 25 (−25) gpm starting at 50 (−50) gpm. The *thick grey line* indicates the climatological winter reference latitude. See text for acronyms

reconciles both approaches is proposed, providing a two-folded complementary perspective of blocking as a signature in the anomalous field capable of reversing the meridional jet-based height gradient in the total flow. This novel approach is also presented as an attempt to pave the way into a definitive blocking definition.

The novel blocking detection method is based on 500 hPa geopotential height data of wide availability in GCMs and high reliability in reanalyses. A reference latitude and an anomaly threshold account for the most characteristic features of blocking, namely the suppression of the jet stream with blockage of storm tracks and its 2-D amplitude, respectively. The simultaneous need for both parameters is compensated by the removal of some artificial assumptions resulting from single blocking indices. Secondary parameters are based on the requirement of temporal persistence, spatial extension and overlapping criteria to the daily detected blocked flows.

Thresholds' calibration of critical parameters has been determined from objectively derived margins that are independent of the type and resolution of the grid used (e.g. by replacing grid-point based thresholds by areal or resolution-dependent criteria) but dependent of the input data (i.e. adjusted from the specific observed or simulated mean climate state) in order to allow the applicability of the method to observational and model studies. A higher amount of arbitrariness is acceptable in the choice of the secondary parameters' thresholds, with an assessment of typical spatial and temporal characteristics of blocking being enough to set appropriate values. The proposed method is of a lagrangian nature since it identifies individual blocking events but simultaneously allows 2-D descriptors of blocking density. As critical thresholds are data-dependent (i.e. they are determined from the specific climate) the method can be applied to long series of data sets, including GCMs with different spatial resolutions.

The proposed index shares some similarities with previous blocking indicators but some discrepancies arise. Thus, unlike single approaches that just highlight preferred blocking regions on the basis of certain signature of the general circulation, the combined index shows a good agreement with the climatological regions of maximum band-pass height variance and wave amplification. Furthermore, a number of atmospheric patterns identified by some previous blocking indices over specific regions do not typically correspond to standard blocking signatures.

Summarizing, there is enough evidence to support that this blocking method conciliates previous blocking definitions through the use of a combined blocking index that avoids artificial assumptions and improves the detection efficiency. Additionally, this method can be applied to different data sets, being useful for observations and model simulations of different resolutions, temporal lengths and time variant basic states. Results suggest the need of caution in objective automatic diagnosis tools if they are to be applied to GCMs, where empirical (i.e. observational) thresholds that are critical for the method may be unsuitable for the climate of the model. These questions will be further addressed in the companion Paper II.

**Acknowledgments** This study received support from MICINN through the TRODIM (CGL2007-65891-C05-05/CLI and CGL2007-65891-C05-02/CLI) projects, from IDL-FCUL through the ENAC (PTDC/AAC-CLI/103567/2008) project and from the EU 6th Framework Program (CIRCE) contract number 036961 (GOCE). We would like to thank J. F. González-Rouco for providing useful comments and suggestions. Two anonymous reviewers contributed to improve the final version of this paper.

## Appendix: Computation of the anomaly field

Assuming that the length of the data set is $K$ years, $N$ the number of data points per year and $M$ the number of data points per month so that $1 \leq t \leq KN$ and $1 \leq \tau \leq N$, a four-step procedure has been applied: (1) evaluation of a running annual mean with special treatment of the ends of the time series (Eq. 5); (2) determination of a running monthly mean of the anomaly relative to the annual mean (Eq. 6); (3) computation of the mean seasonal cycle (Eq. 7); (4) computation of the anomaly field by extracting the annual mean and the seasonal cycle from the total flow (Eq. 8).

$$\overline{z}(t) = \begin{cases} \frac{1}{N+1} \sum_{k=t-N/2}^{k=t+N/2} z(k) & N/2 < t < KN - N/2 \\ \overline{z}(N/2+1) & 1 \leq t \leq N/2 \\ \overline{z}(KN - N/2 - 1) & KN - N/2 \leq t \leq KN \end{cases} \quad (5)$$

$$z*(t) = \begin{cases} \frac{1}{M+1} \sum_{k=t-M/2}^{k=KN-M/2} (z(k) - \overline{z}(k)) & M/2 < t < KN - M/2 \\ z*(M/2+1) & 1 \leq t \leq M/2 \\ z*(KN - M/2 - 1) & KN - M/2 \leq t \leq KN \end{cases} \quad (6)$$

$$\hat{z}(\tau) = \frac{1}{K} \sum_{k=1}^{k=K} z*(N(k-1)+\tau)\, 1 \leq \tau \leq N \quad (7)$$

$$z'(t) = z(t) - \overline{z}(t) - \hat{z}(\tau) \quad 1 \leq \tau \leq N \quad 1 \leq t \leq KN \quad (8)$$

## References

Austin JF (1980) The blocking of middle latitude westerly winds by planetary waves. Q J R Meteorol Soc 106:327–350

Barriopedro D, Garcia-Herrera R, Lupo AR, Hernández E (2006) A climatology of Northern Hemisphere blocking. J Clim 19:1042–1063

Barriopedro D, García-Herrera R, Huth R (2008) Solar modulation of Northern Hemisphere winter blocking. J Geophys Res 113:D14118. doi:10.1029/2008JD009789

Carrera ML, Higgins RW, Kousky VE (2004) Downstream weather impacts associated with atmospheric blocking over the northeast Pacific. J Clim 17:4823–4839

Cash BA, Lee S (2000) Dynamical processes of block evolution. J Atmos Sci 57:3202–3218

Charney JG, DeVore JG (1979) Multiple flow equilibria in the atmosphere and blocking. J Atmos Sci 36:1205–1216

Charney JG, Shukla J, Mo KC (1981) Comparison of a barotropic blocking theory with observation. J Atmos Sci 38:762–779

Chen T-C, Yoon JH (2002) Interdecadal variation of the North Pacific wintertime blocking. Mon Weather Rev 130:3136–3143

Croci-Maspoli M, Schwierz C, Davies HC (2007) Atmospheric blocking: space-time links to the NAO and PNA. Clim Dyn 29:713–725

D'Andrea F et al (1998) Northern Hemisphere atmospheric blocking as simulated by 15 atmospheric general circulation models in the period 1979–1988. Clim Dyn 14:385–407

Diao Y, Li J, Luo D (2006) A new blocking index and its application: blocking action in the northern hemisphere. J Clim 19:4819–4839

Doblas-Reyes FJ, Casado MJ, Pastor MA (2002) Sensitivity of the Northern Hemisphere blocking frequency to the detection index. J Geophys Res 107. doi:10.1029/2000JD000290

Dole RM, Gordon ND (1983) Persistent anomalies of the extratropical northern hemisphere wintertime circulation: geographical distribution and regional persistence characteristics. Mon Weather Rev 111:1567–1586

Elliot RD, Smith TB (1949) A study of the effect of large blocking highs on the general circulation in the northern hemisphere westerlies. J Meteor 6:67–85

García-Herrera R, Barriopedro D (2006) Northern hemisphere snow cover and atmospheric blocking variability. J Geophys Res 111:D21104. doi:10.1029/2005JD006975

García-Herrera R, Paredes D, Trigo RM, Trigo IF, Hernández E, Barriopedro D, Mendes MA (2007) The outstanding 2004–2005 drought in the Iberian Peninsula: impacts and atmospheric circulation associated. J Hydrometeor 8:469–482

Hartmann DL, Ghan SJ (1980) A statistical study of the dynamics of blocking. Mon Weather Rev 108:1144–1159

Huang F, Zhou FX, Qian XD (2002) Interannual and decadal variability of North Pacific blocking and its relationship to SST, teleconnections and storm track. Adv Atmos Sci 19:807–820

Kaas E, Branstator G (1993) The relationship between a zonal index and blocking activity. J Atmos Sci 50:3061–3077

Kalnay E et al (1996) The NCEP/NCAR 40-years reanalyses project. Bull Am Meteor Soc 77:437–471

Knox JL, Hay JE (1984) Blocking signatures in the northern hemisphere: rationale and identification. Atmos Ocean 22:36–47

Knox JL, Hay JE (1985) Blocking signatures in the northern hemisphere: frequency distribution and interpretation. J Clim 5:1–16

Lejenäs H, Økland H (1983) Characteristics of northern hemisphere blocking as determined from long time series of observational data. Tellus 35A:350–362

Liu Q (1994) On the definition and persistence of blocking. Tellus 46A:286–290
Luo D, Wan H (2005) Decadal variability of wintertime North Atlantic and Pacific blockings: a possible cause. Geophys Res Lett 32:L23810. doi:10.1029/2005GL024329
Lupo AR, Smith PJ (1995) Climatological features of blocking anticyclones in the Northern Hemisphere. Tellus 47A:439–456
Masato M, Hoskins BJ, Woollings TJ (2009) Can the frequency of blocking be described by a red noise process? J Atmos Sci 66:2143–2149. doi:10.1175/2008JAS2907.1
Metz W (1986) Transient cyclone-scale vorticity forcing of blocking highs. J Atmos Sci 43:1467–1483
Michelangeli P, Vautard R, Legras B (1995) Weather regime occurrence and quasi stationarity. J Atmos Sci 52:1237–1256
Mullen SL (1986) The local balances of vorticity and heat for blocking anticyclones in a spectral General Circulation Model. J Atmos Sci 43:1406–1441
Mullen SL (1989) Model experiments on the impact of Pacific sea surface temperature anomalies on blocking frequency. J Clim 2:997–1013
Nakamura H, Nakamura M, Anderson JL (1997) The role of high and low frequency dynamics and blocking formation. Mon Weather Rev 125:2074–2093
Namias J (1950) The index cycle and its role in the general circulation. J Meteor 7:130–139
Pelly J, Hoskins B (2003) A new perspective on blocking. J Atmos Sci 60:743–755
Quiroz RS (1984) The climate of 1983–84 winter. A season of strong blocking and severe cold in North America. Mon Weather Rev 112:1894–1912
Rex DF (1950a) Blocking action in the middle troposphere and its effect upon regional climate. Part I: An aerological study of blocking action. Tellus 2:196–211
Rex DF (1950b) Blocking action in the middle troposphere and its effect upon regional climate. Part II: The climatology of blocking action. Tellus 2:275–301
Rex DF (1951) The effect of Atlantic blocking action upon European climate. Tellus 3:1–16
Rossby CG (1939) Relation between the variations in the intensity of the zonal circulation of the atmosphere on the displacement of the semi-permanent centers of action. J Mar Res 2:38–55
Sanders RA (1953) Blocking highs over the eastern North Atlantic ocean and western Europe. Mon Weather Rev 81:67–73
Sausen R, König W, Sielmann F (1995) Analysis of blocking events observation and ECHAM model simulations. Tellus 47A:421–438
Scherrer SC, Croci-Maspoli M, Schwierz C, Appenzeller C (2006) Two-dimensional indices of atmospheric blocking and their statistical relationship with winter climate patterns in the euro-atlantic region. Int J Climatol 26:233–249
Schwierz C, Croci-Maspoli M, Davies HC (2004) Perspicacious indicators of atmospheric blocking. Geophys Res Lett 31:6125–6128
Schwierz C, Appenzeller C, Davies HC, Liniger MA, Muller W, Stocker TF, Yoshimori M (2006) Challenges posed by and approaches to the study of seasonal-to-decadal climate variability. Clim Change 79:31–63
Shukla J, Mo KC (1983) Seasonal and geographical variation of blocking. Mon Weather Rev 111:388–402
Stan C, Straus DM (2007) Is blocking a circulation regime? Mon Weather Rev 135:2406–2413
Sumner EJ (1954) A study of blocking in the Atlantic-European sector of the Northern Hemisphere. Q J R Meteorol Soc 80:402–416
Tibaldi S, Molteni F (1990) On the operational predictability of blocking. Tellus 42A:343–365
Tibaldi S, Tosi E, Navarra A, Pedulli L (1994) Northern and Southern hemisphere seasonal variability of blocking frequency and predictability. Mon Weather Rev 122:1971–2003
Treidl RA, Birch EC, Sajecki P (1981) Blocking action in the Northern Hemisphere: a climatological study. Atmos Ocean 19:1–23
Trenberth KE et al (2007) Observations: surface and atmospheric climate change. In: Solomon S, Qin D, Manning M, Chen Z, Marquis M, Averyt KB, Tignor M, Miller HL et al (eds) Climate change 2007: the physical science basis. Contribution of Working Group I to the Fourth Assessment Report of the Intergovernmental Panel on Climate Change. Cambridge University Press, Cambridge
Trigo RM, Trigo IF, DaCamara CC, Osborn TJ (2004) Winter blocking episodes in the European-Atlantic sector: climate impacts and associated physical mechanisms in the reanalysis. Clim Dyn 23:17–28
Tsou CH, Smith PJ (1990) The role of synoptic/planetary-scale interactions during the development of a blocking anticyclone. Tellus 42A:174–193
Tyrlis R, Hoskins BJ (2008) Aspects of Northern Hemisphere atmospheric blocking climatology. J Atmos Sci 65:1638–1652
Vautard R (1990) Multiple weather regimes over the North Atlantic: analysis of precursors and successors. Mon Weather Rev 118:2056–2081
Verdecchia M, Visconti G, D'Andrea F, Tibaldi S (1996) A neural network approach for blocking recognition. Geophys Res Lett 23:2081–2084
Wang L, Chen W, Zhou W, Chan JCL, Barriopedro D, Huang R (2009) Effect of the climate shift around mid 1970's on the relationship between wintertime Ural blocking circulation and East Asian climate. Int J Climatol. doi:10.1002/joc.1876
Wiedenmann JM, Lupo AR, Mokhov II, Tikhonova EA (2002) The climatology of blocking anticyclones for the Northern and Southern Hemispheres: block intensity as a diagnostic. J Clim 15:3459–3473